Supplemental Material

METHODS

Surgery: Rats were anesthetized with an i.p. injection of ketamine-xylazine-acepromazine mixture (100, 5.2, 1 mg/kg respectively) and supplemented with 30 % of the induction dose as needed. After placement in a stereotaxic device (Narishige, Japan), the scalp was excised and holes were drilled for anchoring screws and electrode bundles. Movable bundles of sixteen microwires (Fontanini et al., 2009; Fontanini and Katz, 2006) were implanted either bilaterally in GC (AP 1.4, ML ± 5 from bregma, DV –4.5 from dura) or unilaterally in GC and BLA (AP -3, ML ± 5.1, DV –7) and cemented in place with dental acrylic. In a subset of rats stainless steel guide cannulae (23 ga) for injections were implanted 1 mm dorsal to BLA. Following electrode and cannulae implantation, a positioning bolt for restraint was implanted in the acrylic cap and IOC were inserted bilaterally and cemented (Fontanini and Katz, 2005; Phillips and Norgren, 1970). All subjects were given at least 7 days for recovery.

BLA inactivation procedures: Rats implanted with injection cannulae were trained to perform the cued, self-administration paradigm. Once the rats were successfully trained, experimental sessions began. A total of 26 sessions were performed on 7 rats. Each session was divided into two sections: a pre-infusion and post-infusion portion. We relied on less trials per taste than the UT/ExpT experiments to keep sessions short and avoid any possible confound emerging from long sessions and interruptions for infusions. In each trial the rat had to self-administer a tastant following the onset of the cue (as described in the methods). No deliveries of unexpected tastants were included in these experiments, which focused exclusively on cue-responses. Upon termination of the first portion, the stylet in the guide cannula was replaced with a 30 ga injection cannula connected to 10 µl Hamilton (Hamilton) syringe via a small length of PE-10 tubing. Injection was controlled by a microinfusion pump. Rats were injected with either 0.2 µl saline (control) or 0.2 µl of the NBQX (5µg/µl), an AMPA receptor antagonist, bilaterally into BLA. Injections took 2 min and were allowed a further 2 min for diffusion (as in (Haney et al., 2010; McDannald et al., 2004)). The second portion of the experiments began approximately 10 min after removing the injection cannula.

Identification of different cell classes. Cue-responsive neurons that did not show somatosensory rhythmicity were classified as putative pyramidal neurons or interneurons according to their

spontaneous firing frequency and the width of their action potentials (Mitchell et al., 2007). The width was measured as the time interval between the negative and the positive peak (**Figure S5**). The distribution of spike widths was computed and its bimodality was established using the Hartigan's dip test. The distribution was fitted with a sum of two Gaussians and the dip between the two Gaussians was used as the boundary value (300 μs). If spike width was larger than 300 μs it was defined as "wide"; if it was shorter than 300 μs it was considered "narrow". Spontaneous firing rate was used as a second parameter for determining the cell class. Neurons with wide spikes and spontaneous firing rates lower than 10Hz were defined as putative pyramidals; whereas neurons with narrow spikes and spontaneous firing rates higher than 10Hz were defined as interneurons. According to these parameters, the population of 58 cue-responsive neurons could be divided into the following sub-populations: putative pyramidals (40 neurons, mean spike width 381 ± 4 μs, mean firing rate 5.0 ± 0.5 Hz), putative interneurons (6 neurons, mean spike width 187 ± 17μs, mean firing rate 29.6 ± 4.6 Hz). 12 neurons could not be classified because they had either wide action potentials and high firing rates (3 neurons, mean spike width 417 ± 22 □s, mean firing rate 16.7 ± 3.0 Hz) or narrow action potentials and low firing rates (8 neurons, mean spike width 197 ± 19 □s, mean firing rate 3.6 ± 0.9 Hz) or because the spike width happened to be at the boundary between our definition of wide and narrow (1 neuron, width: 300 □s). Only putative pyramidal neurons were used for correlation analyses detailed in **Figure 5, panels B-D,** and **Figure 6**.

Analysis of mouth movements and oro-facial behaviors: A randomly chosen subset (n = 11) of the experimental sessions was used for automated video analysis. Videos (30 frames/s) of orofacial behaviors were imported into MATLAB in 8 bit MPEG format. In order to assess the extent to which the mouth moved frame to frame, a crop of the mouth was taken, and both the absolute and non-absolute difference in pixel intensity across consecutive frames was computed. These differences were summed over the whole cropped image providing a single value estimate of orofacial movement over a 33 ms period. Video segments were extracted around cue and tastant presentations,- 1 second before and 2 seconds after. Frames containing near-white pixels, a flag indicating paw movements within the crop, were removed from the analysis. The time course of the intensity difference was averaged across all cue presentations, ExpT and UT within a session. The latency of mouth movements was assessed using an ANOVA and post-hoc analysis across 33 ms time bins around the events. The Tukey-Kramer post-hoc analysis was used to compare two bins prior to each event with 5 bins following. The earliest bin to

show significance from the two bins prior to the event determined the latency of mouth movement. The magnitude of the mouth movements were determined by first finding the peak movement within the first 500 ms following the event (or before the earliest taste delivery for cue presentations), and subtracting the value of the bin prior to that event. Amplitude of movements were measured in the following conditions: before cue (i.e. background), after cue, before ExpT, after ExpT, after UT. All amplitudes were expressed as % of the maximal amplitude evoked by ExpT. Student's t-test were performed to compare amplitude of stimulus-related movements with background movement. Mouth movements were used to infer licking related tongue movements. Lingual movements following infusions from intra-oral cannulae are tightly coupled with mandible opening and closing, as revealed by electromyographic analyses of lingual and anterior digastric muscles (responsible for tongue protrusions and retractions and jaw opening respectively)(Travers and Jackson, 1992; Travers and Norgren, 1986). Automated analysis was validated via blind frame-by-frame visual inspection. Quantification of mouth movements and oro-facial reactions was performed on a subset of 5 randomly chosen experimental sessions. Minimal mouth movements were assessed as the first visible change in position of the mouth following delivery of the tastant. To further classify palatability-related behaviors, three components of oro-facial reactivity were scored: small tongue protrusions, lateral tongue protrusions and gapes. The first two were defined as rhythmic protrusions of the tongue either on the midline beyond the incisor teeth or laterally extending beyond and pushing the lip forward. Wide amplitude openings of the mouth with retraction of the corners were defined as gapes (Fontanini and Katz, 2006; Grill and Norgren, 1978). Each occurrence of the two behaviors were counted for each of the four tastes either expected or unexpected during every video segment. Video scoring was performed blind to taste delivered and condition (UT, ExpT).

Histology: Following the experimental sessions, subjects were terminally anesthetized and intracardially perfused with saline followed by 5 % formalin. DC current (7 µA for 7 s) was passed through selected wires to mark electrodes location. Standard histological procedures (Prussian Blue followed by Cresyl Violet) were used on 80 µm coronal sections to verify electrode and cannula placement.

LEGENDS

Figure S1: Expectation-dependent changes in firing rates. **A.** Pie charts showing all the neurons with different responses to UT and ExpT divided in two populations: neurons in which ExpT evoked an increase of firing rates compared to UT (light blue: ExpT > UT) and those that showed a decrease (pink: UT > ExpT). The plot shows a similar proportion of neurons in the two groups for both the first (0-125 ms left) and second bin (125-250 ms) following stimulus delivery. A minor percentage of neurons had mixed effects that varied for specific tastants (white portion of the pie chart). **B.** Population PSTH in response to ExpT (blue trace) and UT (red trace) for UT > ExpT (top row) and ExpT > UT (bottom row) neurons. The left column shows graphs for the first bin, the right for the second bin (right). The shading around traces represents standard error of mean; time 0 is the delivery of the tastant. **C.** Population PSTH for responses to UT (red trace) and ExpT (blue trace) in all the neurons (n = 298). The shading around each trace represents the standard error of the mean. Note the ramping increase in the firing rates before self-delivery of ExpT. This ramp corresponds to the pre-stimulus difference between UT and ExpT (ΔPSTH) detailed in Figure 2A. As expected on the basis of the results in panel **A** and **B**, the population PSTH for ExpT and UT are similar after stimulus delivery. This occurs because increases and decreases of taste evoked responses were equally split between UT and ExpT, hence resulting in a similar average population PSTH. The absolute difference between PSTH (ΔPSTH) allowed us to appreciate the early difference between responses regardless of its sign (see Figure 1A and 2B). The thick horizontal bars labeled as M (minimal mouth movements), G (gapes), TP (small tongue protrusions) and LTP (lateral tongue protrusions) indicate the average onset time (± standard error of the mean) for each oro-facial reaction in response to UT (red lines) and ExpT (blue lines).

Figure S2: Pre-stimulus anticipatory activity does not occur for uncued and non-tastant delivering lever presses. **A.** Population PSTH in response to cued self-administration (blue trace) and for erroneous lever-presses in the fore-period before the presentation of the cue (green trace) (125 ms bin width, n = 298). The shading around the traces represents the standard error of the mean. Note the absence of ramping activity before erroneous lever presses. Ramping activity is present for cued self-administration. The thick horizontal line on top represents the time points at which the difference between the two traces is significant ($p < 0.5$). **B.** Raster plot and PSTH for a representative neuron. The top plots show responses to cued self-administrations, while bottom plots display activity around

erroneous lever-presses for the same neuron. Magenta diamonds in the top raster indicate onset of the cue.

Figure S3: Onset of cue responses precedes earliest minimal mouth movements. **A.** Average latency of cue responses vs average latency of minimal mouth movements. Each point represents a non-somatosensory cue-responsive neuron, a total of 26 neurons from 10 randomly selected sessions were used for this analysis. Latencies were measured using an automated Matlab routine and blindly validated with frame-by-frame visual inspection of the videos. **B.** Population PSTH aligned to minimal mouth movements (n = 15, bin width = 125 ms). The elevation in firing rate before the onset of the minimal movement confirms that cue responses precede detectable movements. The gray shading represents the standard error of the mean. Dashed line: background firing rate. **C.** Representative PSTH in response to cues (left) and minimal mouth movements (right). Orange diamonds: timing of the minimal mouth movement; magenta diamonds: onset of the cue; blue diamonds: time of self-delivery. The top row shows an example of an excitatory response; the bottom row displays an inhibitory response. Visual inspection of these representative examples confirms that cue responses are fast and their onset precedes that of minimal mouth movements.

Figure S4: Representative responses to cues in three simultaneously recorded BLA neurons. Each panel shows a raster plot (top) and a PSTH (bottom) in response to anticipatory cues (t = 0). Blue diamonds represent the time of self-administration. The figure details three simultaneously recorded neurons, two (left and right panel) that produced excitatory responses to the cue and one (middle) with an inhibitory response.

Figure S5: Correlation between firing rates in response to the cue (x-axis) and to UT (y-axis) in different sub-populations of cue-responsive neurons. Responses are limited to the first 125 ms following the stimulus. **A.** Firing rates of the entire population of cue-responsive neurons that do not show the rhythmic somatosensory signature (n = 58). **B.** Analysis of the width of spike waveforms for all the neurons featured in panel A. The histogram in the left panel presents the distribution of spike widths. The distribution is bimodal (Hartigan's dip test, $p < 0.01$) and can be fitted with a sum of two Gaussians (solid overlaying line). Blue bars indicate wide spike waveforms; red bars indicate narrow spike waveforms. The single gray bar represents a non-classified intermediate width. The top right panel

shows representative average waveforms for two neurons (blue: neuron with wide spikes; red: neuron with narrow spikes). The shading indicates the standard error of the mean. Dotted lines mark the points used for measuring the width (negative and positive peak). The bottom right panel shows all the large (blue) and narrow (red) average waveforms. **C.** This plot shows the correlation between firing rates in response to the cue (x-axis) and to UT (y-axis) for different sub-populations of neurons. Sub-populations were determined on the basis of spike width and spontaneous firing rates. Neurons with wide spike waveforms (i.e. > 300 ?s) and spontaneous firing rates less than 10Hz were defined as putative pyramidal (blue dot, pyr; n = 40). Neurons with narrow spike waveforms (i.e. < 300 ?s) and spontaneous firing rates higher than 10Hz were defined as putative interneurons (red triangle, inter; n = 6). Neurons with either wide spike waveforms and spontaneous firing rates higher than 10Hz (gray dots, pyr wf-high ff; n = 3) or narrow spike waveform and spontaneous firing rats lower than 10Hz (gray triangles, inter wf-high ff; n = 8) or with intermediate spike width (gray square, 300 ?s; n = 1) were deemed too ambiguous to be classified.

Figure S6: Correlation analysis and PCA on the entire population of cue-responsive neurons with no somatosensory rhythmicity (n=58). **A.** Trial-averaged running correlation between the population firing patterns evoked by the cue in the first 125 ms and the time course of the population response to UT. The z-score was used to normalize firing rates. The shaded area around the trace represents the standard error of the mean. The asterisk indicates that the correlation value for the first bin significantly exceeds all the others ($p < 0.05$). **B.** PCA based visualization of the population activity in response to the cue (blue line and dots) and unexpected tastants (black line and dots); numbers indicate the order of 125 ms wide bins following stimulation. **C.** Trial averaged running correlation between population activity evoked by ExpT in the first 125 ms and the time course of the average response to UT. As in **A** the z-score was used to normalize firing rates. The shading around the line represents the standard error of the difference. The dashed box highlights the wide correlation with the first and second bin after UT. **D.** PCA based visualization of population activity evoked by expected (gray) and unexpected (black) tastants. **E.** Trial-averaged running correlation for individual tastants confirms the same patterns as in panel A. The color coded dashed lines represents the data for each tastant (S = Sucrose - blue; Na = NaCl 0 cyan; CA = Citric Acid - yellow; Q = Quinine - red). Gray solid line: average running correlation of the four tastants. The dashed box highlights the wide correlation

with the first and second bin after UT. **F.** PCA analysis for individual tastants. As in **D** the gray line represents ExpT and the black line UT.

Figure S7: Time-course of mouth movements in response to cues, ExpT and UT. **A.** Mouth movements measured using an automated Matlab routine for video analysis. The script performs a frame-by-frame and pixel-by-pixel subtraction of pixel intensity within a region of interest (i.e. mouth). The results of this analysis for movements evoked by cues, ExpT and UT are detailed in the top, middle and bottom row respectively. Left column: representative result for a single trial; middle column: the same trial as above, but rectified to better assess absolute movements; right column: average rectified difference for the entire representative session. Shading around the trace represents standard error of the mean. Each trace has a bin width of 30 ms. **B.** Analysis of latency and amplitude of mouth movements. The left panel shows the latency of mouth movements evoked by cues, ExpT and UT: 188.66 ± 30.48 ms, 66.47 ± 4.22 ms and 95.67 ± 6.13 ms respectively (n = 10). The latency evoked by ExpT is ~29 ms shorter than for UT ($p < 0.01$). Both, ExpT and UT, evoke movements with a significantly faster onset than cues ($p < 0.05$). The right panel compares the amplitude of mouth movements evoked by cues, ExpT, and UT. Cues evoke mouth movements that are significantly smaller than those evoked by tastants. Mouth movements in the 125 ms prior to self-delivery have an amplitude that is only 12.7 % of that of movements evoked by tastants. The asterisk indicates significant differences.

Table S1: Analysis of oro-facial reactions (tongue protrusions and gapes) in response to expected and unexpected tastants. Overall ExpT appear to be more palatable and less aversive than UT. Indeed they evoke significantly more tongue protrusions and less gapes than UT. NaCl, Citric Acid and Quinine evoke significantly less gapes when expected; NaCl and Quinine evoke significantly more tongue protrusions when expected. The effects of expectation on the latency of oro-facial reactions vary: while gapes and lateral tongue protrusions have the same onset regardless of whether the tastant was expected or not, small tongue protrusions occurred earlier when the stimulus was expected.

REFERENCES

Fontanini, A., Grossman, S.E., Figueroa, J.A., and Katz, D.B. (2009). Distinct subtypes of basolateral amygdala taste neurons reflect palatability and reward. J Neurosci *29*, 2486-2495.

Fontanini, A., and Katz, D.B. (2005). 7 to 12 Hz activity in rat gustatory cortex reflects disengagement from a fluid self-administration task. J Neurophysiol *93*, 2832-2840.

Fontanini, A., and Katz, D.B. (2006). State-dependent modulation of time-varying gustatory responses. J Neurophysiol *96*, 3183-3193.

Grill, H.J., and Norgren, R. (1978). The taste reactivity test. I. Mimetic responses to gustatory stimuli in neurologically normal rats. Brain Res *143*, 263-279.

Haney, R.Z., Calu, D.J., Takahashi, Y.K., Hughes, B.W., and Schoenbaum, G. (2010). Inactivation of the central but not the basolateral nucleus of the amygdala disrupts learning in response to overexpectation of reward. J Neurosci *30*, 2911-2917.

McDannald, M., Kerfoot, E., Gallagher, M., and Holland, P.C. (2004). Amygdala central nucleus function is necessary for learning but not expression of conditioned visual orienting. Eur J Neurosci *20*, 240-248.

Mitchell, J.F., Sundberg, K.A., and Reynolds, J.H. (2007). Differential attention-dependent response modulation across cell classes in macaque visual area V4. Neuron *55*, 131-141.

Phillips, M.I., and Norgren, R. (1970). A rapid method for permanent implantation of an intraoral fistula in rats. Behavioral Research, Methods, & Instrumentation, 124.

Travers, J.B., and Jackson, L.M. (1992). Hypoglossal neural activity during licking and swallowing in the awake rat. J Neurophysiol *67*, 1171-1184.

Travers, J.B., and Norgren, R. (1986). Electromyographic analysis of the ingestion and rejection of sapid stimuli in the rat. Behav Neurosci *100*, 544-555.

Supp Figure 1

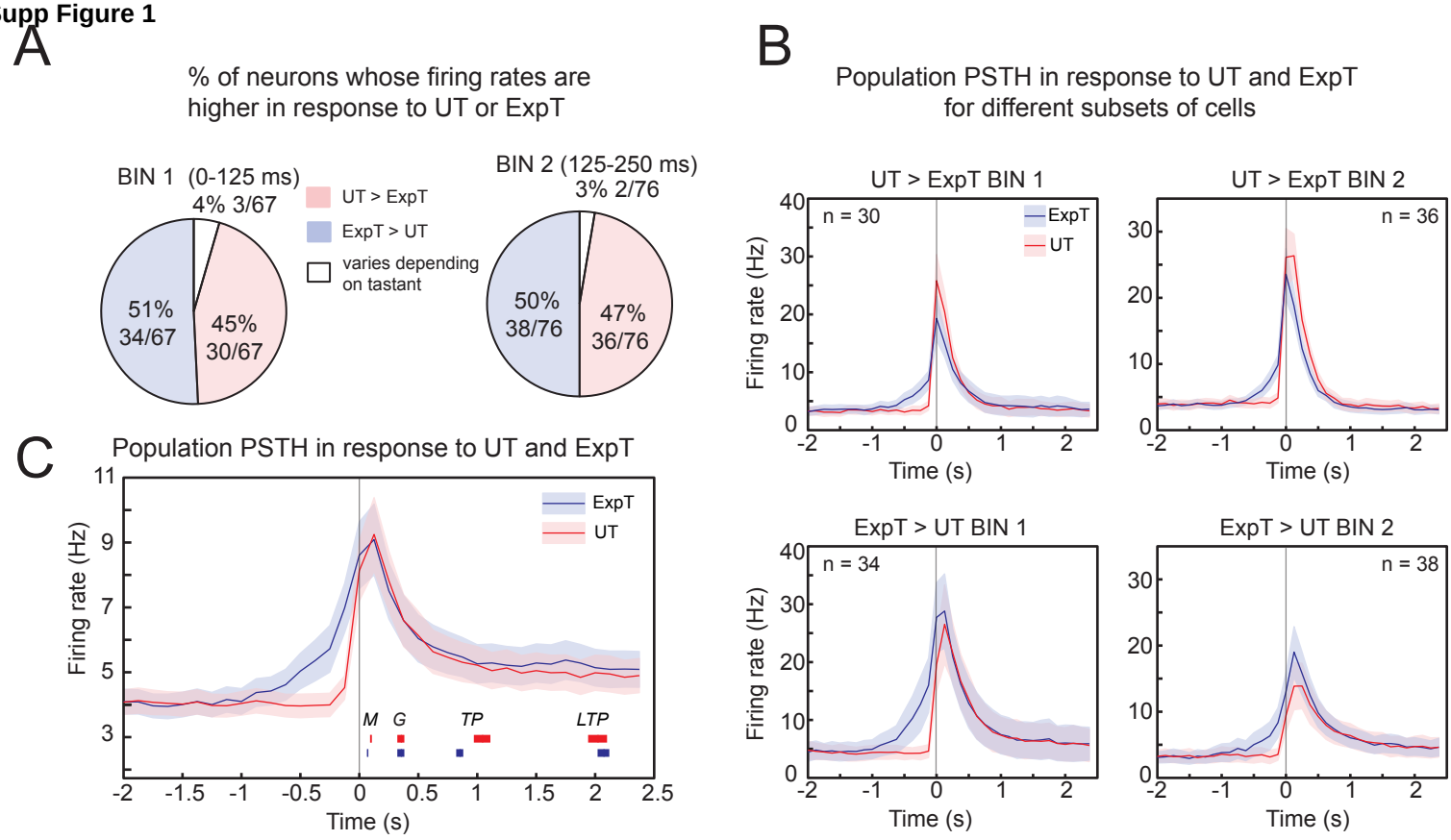

Supp Figure 2

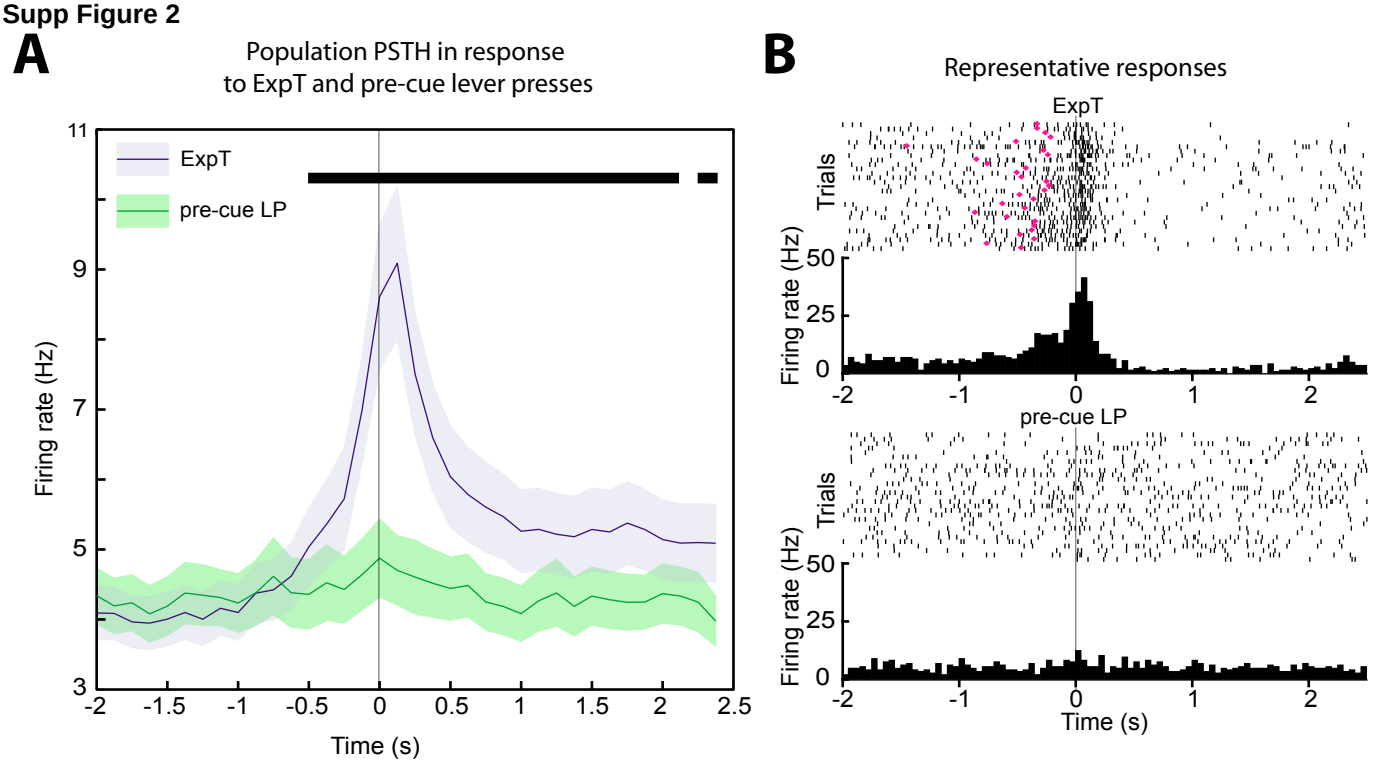

Supp Figure 3

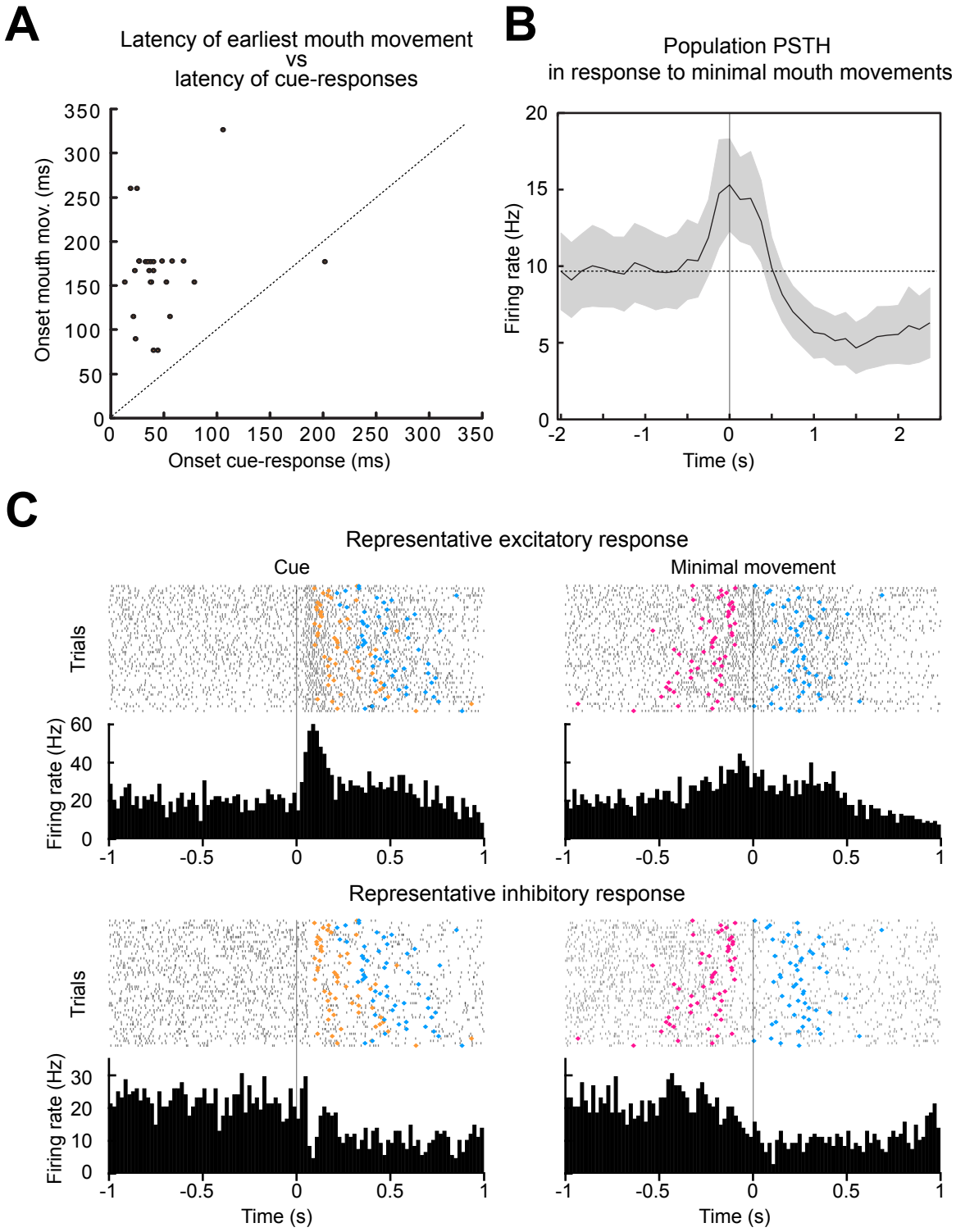

Supp Figure 4

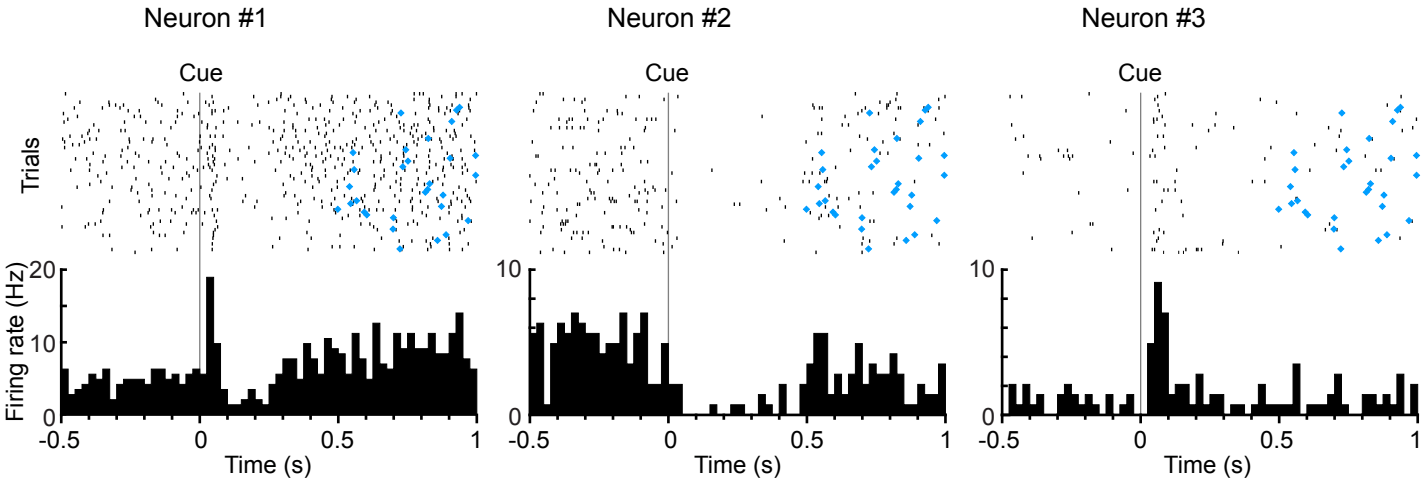

Supp Figure 5

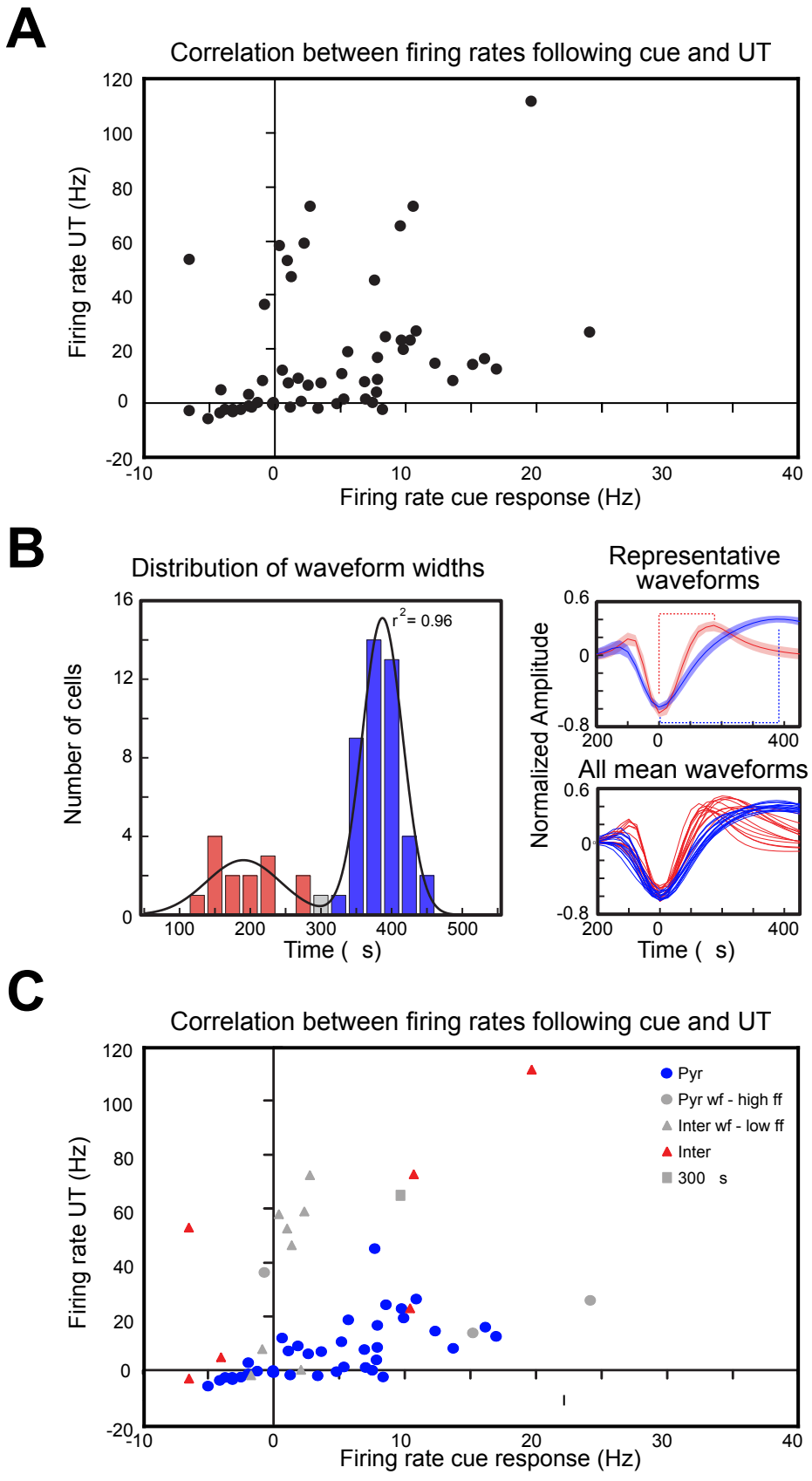

Supp Figure 6

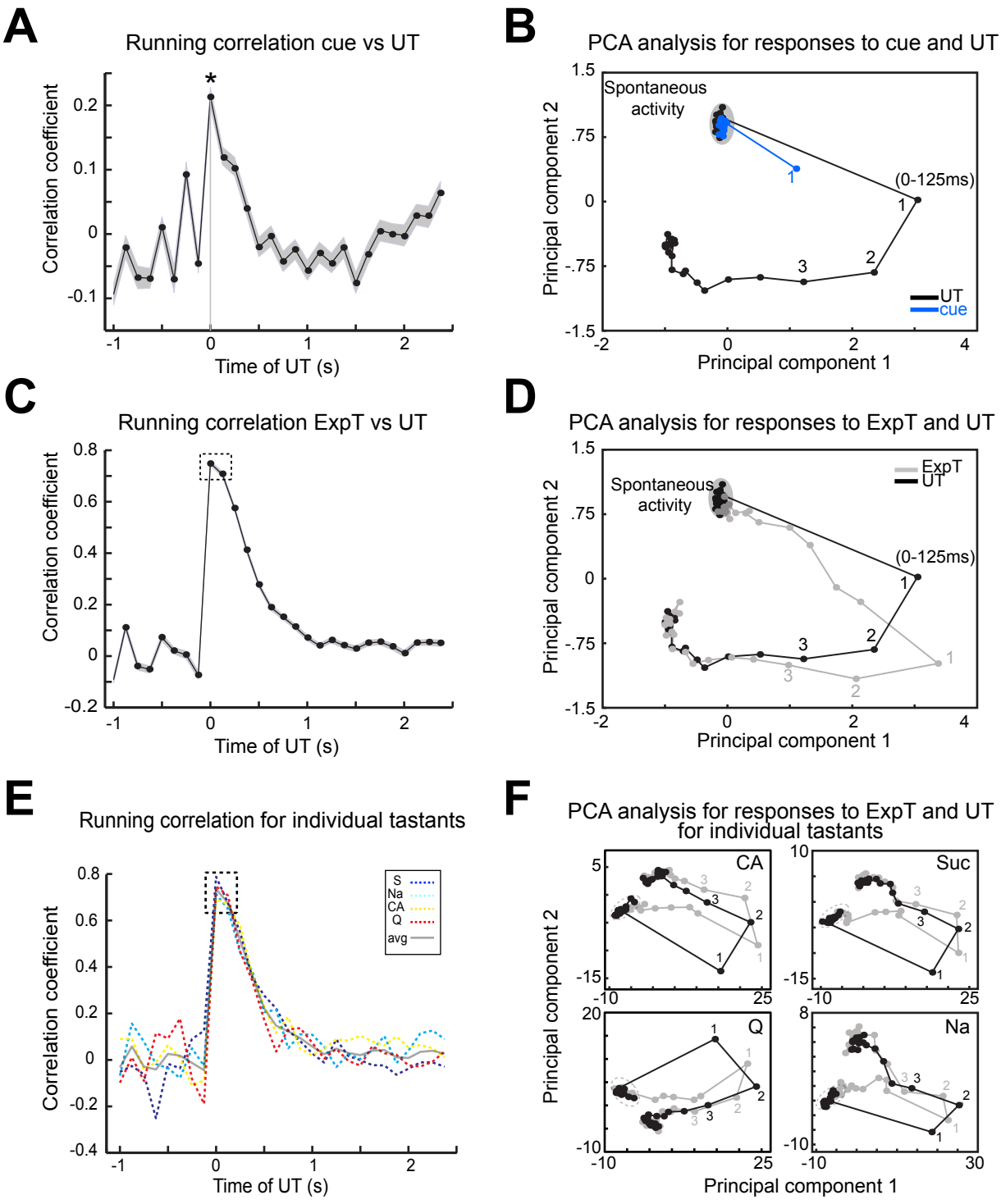

Supp Figure 7

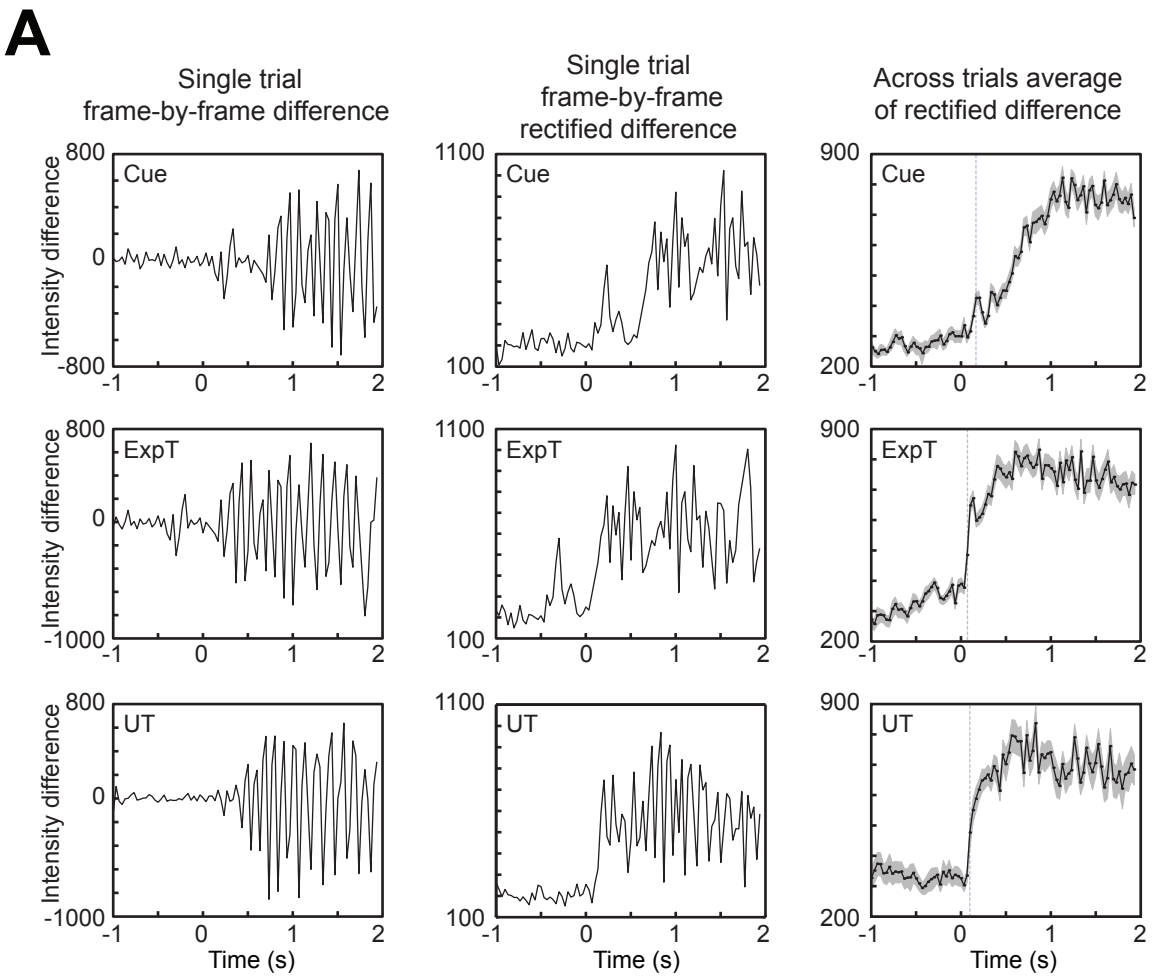

Supp Table 1

Total oro-facial reactions (tongue protrusions and gapes)		
	# tongue protrusions	**# gapes**
Expected	13.27 ± 0.40 ($p < 0.01$)	0.24 ± 0.04
Unexpected	10.65 ± 0.58	0.58 ± 0.09 ($p < 0.01$)

Number of gapes by taste				
	Sucrose	**NaCl**	**Citric Acid**	**Quinine**
Expected	0.09 ± 0.04	0.05 ± .02	0.20 ± 0.05	0.61 ± 0.15
Unexpected	0.15 ± 0.06	0.21 ± 0.09 ($p < 0.05$)	0.44 ± 0.13 ($p < 0.05$)	1.46 ± 0.28 ($p < 0.01$)

Number of tongue protrusions by taste				
	Sucrose	**NaCl**	**Citric Acid**	**Quinine**
Expected	12.48 ± 0.69	12.21 ± 0.70 ($p < 0.05$)	17.34 ± 0.97	10.76 ± 0.59 ($p < 0.01$)
Unexpected	10.86 ± 0.91	9.55 ± 1.03	15.92 ± 1.41	6.41 ± 0.68

Latency of orofacial reactions (ms)			
	Gapes	**Small Tongue Protrusions**	**Lateral Tongue Protrusions**
Expected	350 ± 30	850 ± 30	2070 ± 50
Unexpected	350 ± 30	1040 ± 70 ($p < 0.05$)	2020 ± 80